Journal of Information Systems Engineering and Management
2025, 10(4)
e-ISSN: 2468-4376
https://www.jisem-journal.com/

Research Article

Estimation of Direct and Diffuse Solar Radiation Components from Global Solar Radiation Using CNN-LSTM Hybrid Model

Thameur Obeidi[1, *], Benalia M'hamdi[2], Taieb Iliass[1], Bakhti Damani[1]
[1] *Faculty of Science and Technology, Ziane Achour University, 17000, Djelfa, Algeria.* t.obeidi@univ-djelfa.dz
[2] *Laboratory of Applied Automation and Industrial Diagnostics (LAAID), Faculty of Science and Technology, Ziane Achour University, 17000, Djelfa, Algeria*

ARTICLE INFO

Received: 15 Nov 2024
Revised: 26 Dec 2024
Accepted: 24 Jan 2025

ABSTRACT

This study presents a hybrid deep learning approach utilizing Convolutional Neural Networks (CNN) and Long Short-Term Memory networks (LSTM) to estimate Direct Normal Radiation (DNR) and Diffuse Solar Radiation (DSR) from Global Solar Radiation (GSR). Leveraging temporal patterns and spatial dependencies in solar radiation data, the proposed model aims to provide accurate predictions of solar components critical for solar energy systems. Our model is trained and validated using a real-world dataset comprising daily solar radiation measurements. The CNN-LSTM model outperforms traditional machine learning methods in both accuracy and robustness.

Keywords: Solar radiation, renewable energy, estimation, CNN, LSTM, CNN-LSTM, hybrid model.

INTRODUCTION

Solar radiation and daylight are vital for sustaining life on Earth. They play a key role in shaping the Earth's meteorological patterns and driving renewable energy systems. Estimating the amount of solar radiation reaching the Earth's surface is thus essential for energy planning, environmental studies, and climate modeling [1-5].

In many regions, direct measurements of solar radiation are unavailable due to the high cost and limited coverage of instruments like pyranometers, solarimeters, and pyrheliometers. Additionally, inaccuracies in sensors and missing data further complicate reliable assessments. As a result, researchers have developed various models to estimate global solar radiation (GSR), including empirical, physical, and soft computing approaches [6-10].

In recent years, artificial intelligence (AI) and machine learning (ML) techniques—such as Artificial Neural Networks (ANN)[11-15], Support Vector Machines (SVM), Extreme Learning Machines (ELM)[16-20], and Gaussian Process Regression (GPR)—have been widely applied for solar radiation modeling. Many of these models use meteorological parameters such as air temperature, sunshine duration, humidity, and wind speed as inputs. Studies conducted across diverse locations have shown that ANN-based models, in particular, can yield high accuracy even when only limited meteorological data are available, Table 1 provides an overview of relevant prior work.

In this work, we propose a data-driven approach for estimating the direct normal radiation (DNR) and diffuse solar radiation (DSR) components from GSR, using only the day-of-the-year (DOY) as input. This approach eliminates the need for meteorological parameters and simplifies the prediction process [21-23].

To this end, we develop and compare two deep learning models: the Convolutional Neural Network (CNN) and the Long Short-Term Memory (LSTM) network. While CNNs are known for their ability to extract local patterns and features, LSTMs are effective at learning long-term dependencies in time series. Both models are trained on measured data collected from the Ghardaïa region (Algeria) during 2013–2014 and tested on 2015 data. Their performances are compared using standard metrics to determine the most effective architecture for solar radiation component estimation using a minimal input feature set.

Journal of Information Systems Engineering and Management
2025, 10(4)
e-ISSN: 2468-4376
https://www.jisem-journal.com/

Research Article

The remainder of the paper is organized as follows: Section 2 outlines the theoretical background of CNN, LSTM, and other relevant methods. Section 3 describes the study site and dataset. Section 4 presents results and discussions. Finally, Section 5 concludes the study and provides suggestions for future work.

Table.1 Summary of Related Work

Author(s)	Method(s) Used	Input Parameters	Target	Location	Key Results
Behrang & Assareh [24]	ANN	T, RH, SS, EV, WS	GSR	Iran	Developed two ANN models with meteorological inputs.
Rahimikhoob [25]	ANN	Air temperature	GSR	Semi-arid region	Accurate GSR estimation using limited inputs.
Yadav & Chandel [26]	ANN	SS, T_max, Month, SS_theoretical	GSR	India	Trained 7 ANN models; best performance with 4 inputs.
Rehman & Ohandes [27]	ANN	T, RH	GSR	Abha, Saudi Arabia	ANN estimated GSR accurately with only T and RH.
Lam et al. [28]	ANN	Sunshine Duration	GSR	40 Chinese Cities	$R^2 \geq 0.82$ across different climate zones.
Asl et al. [29]	ANN	Various (not specified)	GSR	Dezful, Iran	APE = 6.08%
Ramedani et al. [30]	MLP Neural Network	T_max, RH, SS, Precipitation	GSR	Tehran, Iran	RMSE = 3.09
Mellit & Pavan [31]	MLP Neural Network	Daily avg GSR, T_avg	GSR	Trieste, Italy	Optimal config: 3 inputs, 2 hidden layers, 24 outputs.
Voyant et al. [32]	ANN	Endogenous + exogenous data	GSR	Corsica, France	Relative RMSE: 0.5% and 1%
Koca et al. [33]	ANN	Latitude, Longitude, Altitude, Month, SS, Cloud	GSR	Turkey	Compared models with different numbers of inputs.
This Work (Proposed)	CNN, LSTM	Day-of-Year (DOY)	DNR, DSR	Ghardaïa, Algeria	Comparison of CNN and LSTM with minimal input (DOY).

.

METHODOLOGY

Data Description

The study utilizes a dataset comprising daily solar radiation measurements collected over multiple days. The key variables include:

- **Day of Year (DOY)**: Sequential day count (1–365/366) to capture seasonal variations.
- **Global Solar Radiation (GSR)**: Total solar energy received on a horizontal surface (Wh/m^2).
- **Direct Normal Radiation (DNR)**: Beam radiation received perpendicular to the sun's rays (Wh/m^2).
- **Diffuse Solar Radiation (DSR)**: Scattered solar radiation due to atmospheric conditions (Wh/m^2).

Data Preprocessing

To enhance model performance, the following preprocessing steps were applied:

- **Normalization**: All radiation values were scaled to a [0, 1] range using min-max normalization to ensure uniform feature weighting [34].

Journal of Information Systems Engineering and Management
2025, 10(4)
e-ISSN: 2468-4376
https://www.jisem-journal.com/

Research Article

- **Windowing**: A sliding window approach generated sequential input-output pairs, capturing temporal dependencies in GSR data [35].
- **Splitting**: The dataset was partitioned into training (70%), validation (15%), and testing (15%) subsets to facilitate robust model evaluation [36].

Convolutional Neural Network (CNN) Architecture

Originally developed for computer vision tasks [37,38], Convolutional Neural Networks have demonstrated remarkable versatility in time-series forecasting applications. Their effectiveness has been particularly notable in energy prediction systems [39], photovoltaic system optimization [40], and renewable energy applications [41], as well as in pattern recognition domains such as speech and facial recognition [42].

The fundamental CNN structure employs a hierarchical feature extraction approach through:

1. **Convolutional Layers**: These apply trainable filters to detect local temporal or spatial patterns
2. **Pooling Layers**: Which progressively reduce feature map dimensionality while preserving essential information [43]
3. **Fully Connected Layers**: That integrate extracted features for final predictions [44,45]

A distinctive strength of CNNs lies in their capacity for automated feature learning, significantly reducing the need for manual feature engineering while enabling robust end-to-end training [46-48]. For photovoltaic power forecasting specifically, CNNs excel at identifying:

- Localized temporal dependencies in irradiation patterns
- Short-term fluctuations in solar energy availability
- Non-linear relationships between meteorological variables and power output

The schematic representation of our implemented CNN architecture appears in Figure 1. This configuration was specifically optimized for solar radiation prediction through extensive hyperparameter tuning and validation testing.

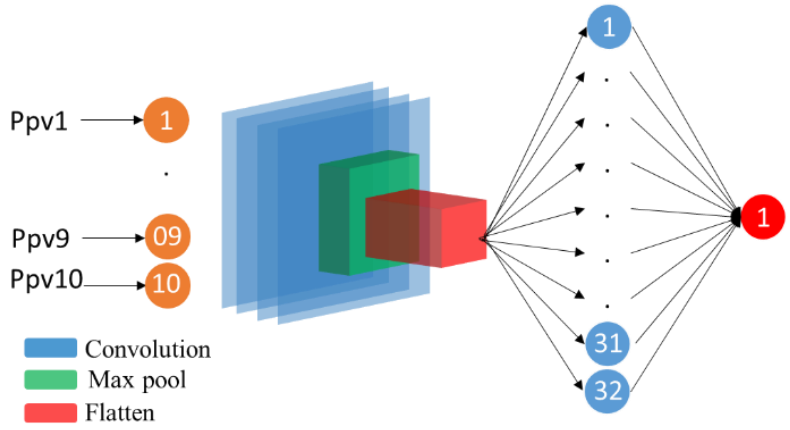

Figure 1. CNN architecture

Long Short-Term Memory (LSTM) Architecture

Long Short-Term Memory networks, first proposed by Hochreiter and Schmidhuber [47], represent an advanced variant of Recurrent Neural Networks (RNNs) specifically engineered to overcome the vanishing gradient problem inherent in conventional RNN architectures. The LSTM's distinctive gating mechanism enables exceptional performance in modeling long-range temporal dependencies, making it particularly suitable for sequential data analysis and time-series forecasting applications.

The fundamental building block of an LSTM network consists of:

Memory Cell: Maintains state information across arbitrary time intervals

Gating Mechanisms:

- Input Gate: Regulates the flow of new information into the cell state

Journal of Information Systems Engineering and Management
2025, 10(4)
e-ISSN: 2468-4376
https://www.jisem-journal.com/

Research Article

- Forget Gate: Determines which historical information to retain or discard
- Output Gate: Controls the cell state's influence on hidden outputs [49,50]

This sophisticated architecture provides three key advantages for solar forecasting:

1. **Selective Memory Retention**: The network can automatically learn which temporal patterns are relevant for prediction
2. **Long-Term Dependency Modeling**: Maintains information over hundreds of time steps without signal degradation
3. **Adaptive Learning**: Dynamically adjusts to varying patterns in seasonal and diurnal solar cycles

The complete LSTM cell architecture implemented in our study is illustrated in Figure 2, with the following implementation details:

- Peephole connections were evaluated but not implemented due to computational constraints
- Coupled input/forget gates were tested for model simplification
- Gradient clipping (norm=1.0) was applied during training for stability
- Layer normalization was incorporated to accelerate convergence

The LSTM's demonstrated capability to capture complex temporal patterns in solar radiation data makes it particularly valuable for both short-term (hourly) and medium-term (daily) forecasting applications.

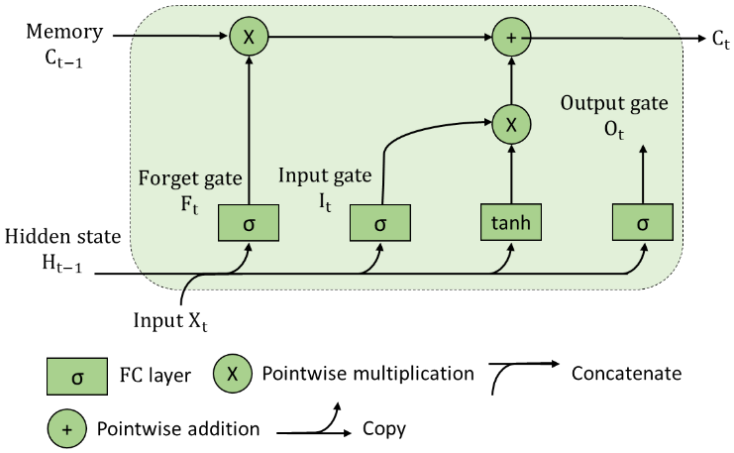

Figure 2. LSTM architecture.

Hybrid CNN-LSTM Architecture

The CNN-LSTM architecture represents a powerful hybrid model that synergistically combines the strengths of convolutional and recurrent neural networks for enhanced time-series forecasting. This architecture has demonstrated superior performance in various temporal prediction tasks by effectively capturing both local patterns and long-term dependencies in sequential data [51,55].

Architecture Overview:

1. **Convolutional Front-End:**
    - Multiple 1D convolutional layers extract hierarchical local features
    - Kernel sizes optimized to capture relevant temporal patterns (typically 3-5 timesteps)
    - ReLU activation functions introduce non-linearity
    - Max-pooling layers reduce dimensionality while preserving essential features

Journal of Information Systems Engineering and Management
2025, 10(4)
e-ISSN: 2468-4376
https://www.jisem-journal.com/

Research Article

2. **LSTM Backbone:**
    - Processed features are fed into LSTM layers for temporal modeling
    - Multiple LSTM layers enable learning at different time scales
    - Dropout layers (p=0.2-0.5) between LSTM units prevent overfitting
    - Optional bidirectional processing captures both forward and backward dependencies

Model Architecture Diagram

The following block diagram (figure .3) illustrates the structure of the CNN and LSTM-based prediction models:

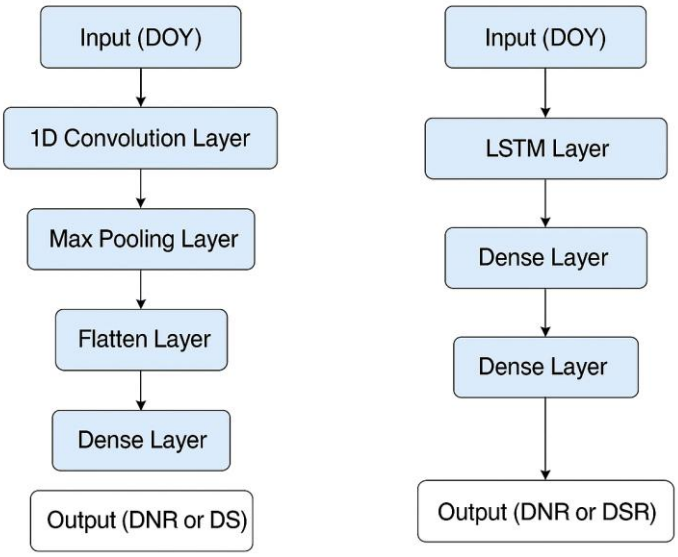

Figure .3 structure of the CNN and LSTM-based prediction models

STUDY AREA AND DATA COLLECTION

Ghardaïa, a Saharan city situated approximately 600 km south of Algeria's capital, lies in an arid and dry region (Figure 4). Its geographic coordinates are 32° 36′ N latitude, 3° 48′ E longitude, and an elevation of 450 meters above mean sea level. The area experiences exceptionally high solar exposure, with annual sunshine exceeding 3,000 hours and an average global solar radiation surpassing 6,000 Wh/m² on a horizontal surface. However, winters in Ghardaïa are notably harsh, with cold winds carrying snow from nearby highlands. Toward the end of winter, sandstorms originating from the southwest bring intense dust, often causing significant disruptions. Summers are extremely hot, with temperatures rising above 45°C, while winters remain relatively cool. Precipitation is scarce and minimal [56-60].

Journal of Information Systems Engineering and Management
2025, 10(4)
e-ISSN: 2468-4376
https://www.jisem-journal.com/

Research Article

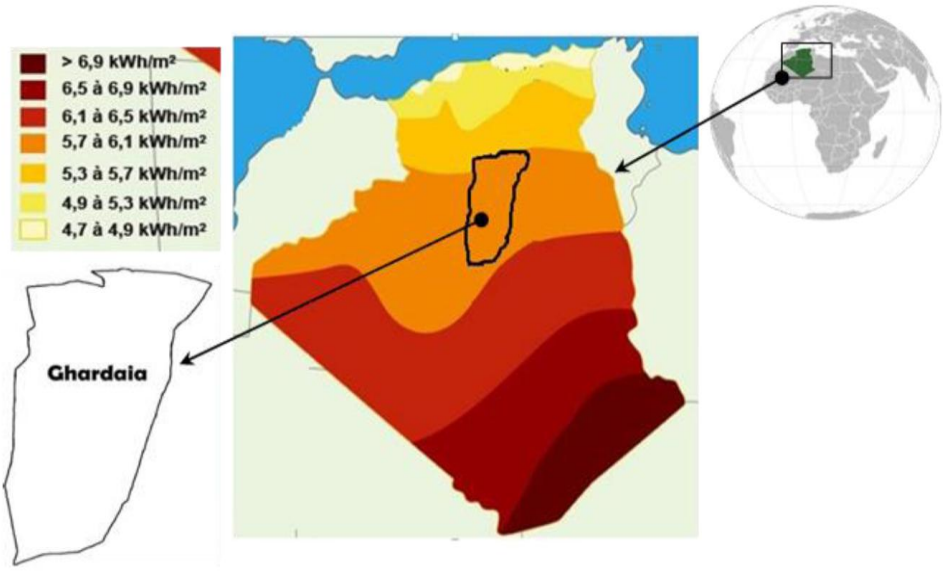

Figure 4. Location of the study area

Ground-based measurements were collected using two ventilated CMP21 Secondary Standard pyranometers from Kipp & Zonen, installed on a SOLYS2 solar tracker equipped with a sun sensor, along with a CHP1 First Class pyrheliometer (Figure 5). These instruments are part of the enerMENA meteorological network, which operates across the Middle East and North Africa (MENA) region.
Figures 6–8 illustrate the daily variations in total GSR, DSR, and DNR for the Ghardaïa region.

Figure 5. Instrumentation station for measuring the global, the direct and the diffuse solar radiation: (1) Pyranometre for measuring the diffuse. (2) irradiance Pyranometre for measuring the global solar irradiance. (3) Peryheliometer for measuring the directirradiance component. (4) The ball used to permanently hide the Pyranometer.

Journal of Information Systems Engineering and Management
2025, 10(4)
e-ISSN: 2468-4376
https://www.jisem-journal.com/

Research Article

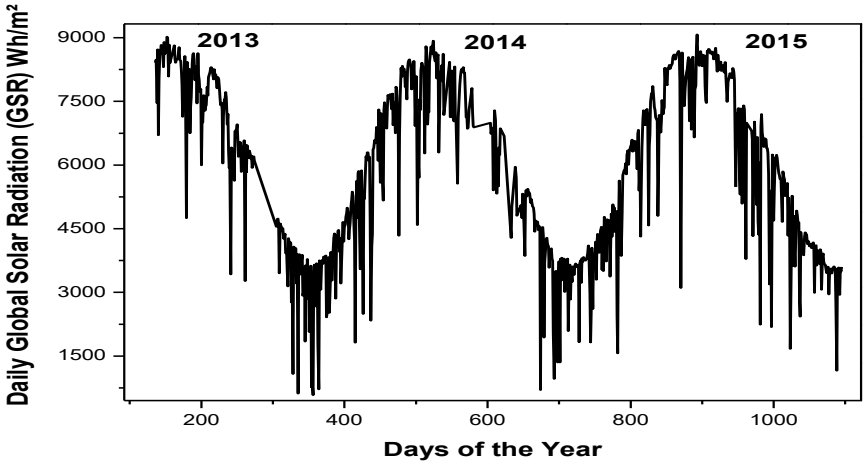

Figure 6. Variation of daily global solar radiation (GSR).

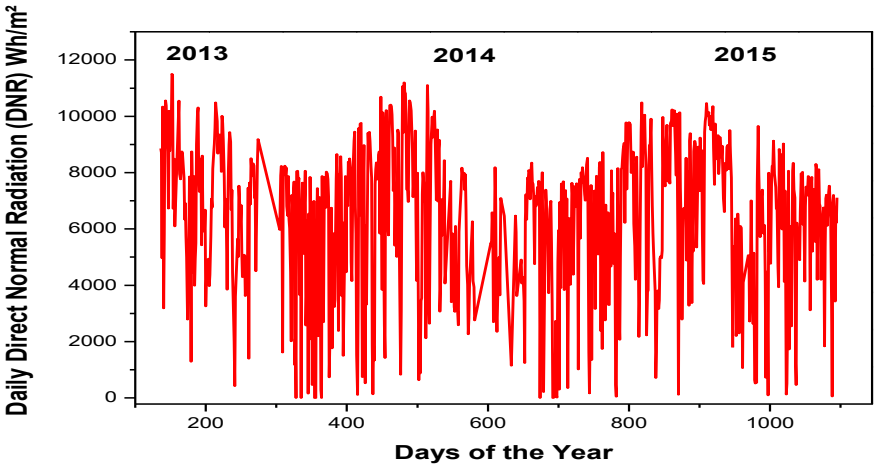

Figure 7. Variation of daily direct normal radiation (DNR).

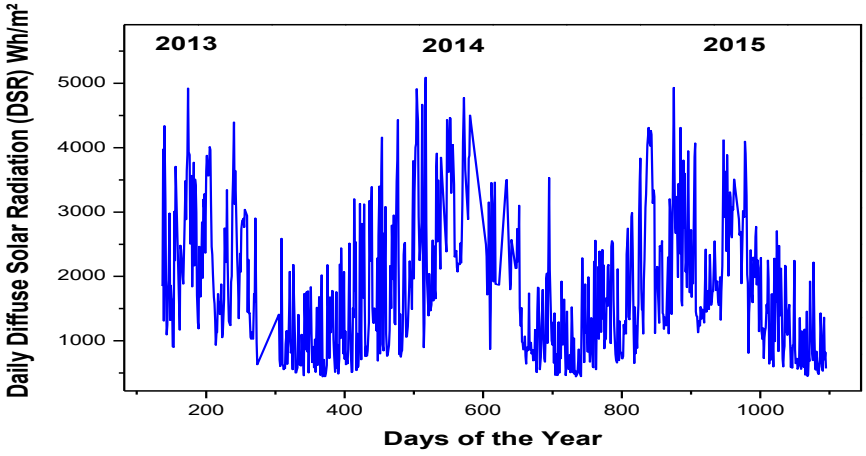

Figure 8. Variation of daily diffuse solar radiation (DSR).

Journal of Information Systems Engineering and Management
2025, 10(4)
e-ISSN: 2468-4376
https://www.jisem-journal.com/

Research Article

MODELS VALIDATION

Although the mathematical formulations of common error metrics can be found in previous studies [61,62], this section highlights their physical interpretation and the improvements they provide.
In this work, six statistical metrics are used to evaluate the forecasting performance of the models: RMSE, MAE, normalized RMSE (nRMSE), normalized MAE (nMAE), the Coefficient of Determination (R2), and the Correlation Coefficient (R).
These metrics offer a comprehensive and scale-independent evaluation of model accuracy, allowing for effective comparison across different algorithms.

Root Mean Square Error (RMSE)

The Root Mean Square Error (RMSE) measures the standard deviation of prediction errors, giving greater weight to larger errors. It is defined as:

$$RMSE = \sqrt{\frac{1}{n}\sum_{i=1}^{n}(H_E - H_M)^2} \tag{10}$$

where:

- H_E is the estimated (predicted) value,
- H_M is the measured (actual) value,
- n is the total number of samples.

Lower RMSE values indicate better forecasting performance.

Mean Absolute Error (MAE)

The Mean Absolute Error (MAE) quantifies the average magnitude of errors in a set of predictions, without considering their direction. It is given by:

$$MAE = \frac{1}{n}\sum_{i=1}^{n}|H_E - H_M| \tag{1}$$

Unlike RMSE, MAE treats all errors equally, providing a direct measure of prediction accuracy.

Normalized RMSE (nRMSE)

The normalized RMSE (nRMSE) expresses the RMSE as a percentage of the mean of the measured values, providing a scale-independent measure:

$$nRSME = \left(\frac{RMSE}{H_{Max} - H_{Min}}\right) \times 100 \tag{2}$$

The ranges of nRMSE define the model performance as [63,64]:
Excellent if: nRMSE $< 10\%$
Good if: $10\% <$ nRMSE $< 20\%$
Fair if: $20\% <$ nRMSE $< 30\%$
Poor if: nRMSE $> 30\%$

Normalized MAE (nMAE)

Similarly, the normalized MAE (nMAE) relates the MAE to the mean of the measured values:

$$nMAE = \left(\frac{MAE}{\frac{1}{n}\sum_{i=1}^{n} H_M}\right) \times 100 \tag{3}$$

This metric also provides a percentage error independent of the data scale.

Coefficient of Determination (R2)

The Coefficient of Determination (R2) assesses how well the predicted values approximate the actual data. It is defined by [65,66]:

Journal of Information Systems Engineering and Management
2025, 10(4)
e-ISSN: 2468-4376
https://www.jisem-journal.com/

Research Article

$$R^2 = 1 - \frac{\sum_{i=1}^{n}(H_M - H_E)^2}{\sum_{i=1}^{n}(H_M - \bar{H}_M)^2} \quad (4)$$

Where $\bar{H}_M$ is the mean of the measured values.
An R^2 value closer to 1 indicates a stronger fit between the predicted and observed data.

Correlation Coefficient (R)
The Pearson Correlation Coefficient RRR quantifies the linear relationship between the predicted and measured values [67-70]:

$$R = \frac{\sum_{i=1}^{n}(H_E - \bar{H}_E).(H_M - \bar{H}_M)}{\sqrt{\sum_{i=1}^{n}(H_E - \bar{H}_E).\sum_{i=1}^{n}(H_M - \bar{H}_M).}} \quad (5)$$

Where $\bar{H}_E$ and $\bar{H}_M$ are the mean predicted and measured values, respectively. An R value close to 1 signifies a strong positive correlation.

RESULTS AND DISCUSSION

Simulation was conducted using each of the three architectures—CNN, LSTM, and CNN-LSTM—on the same dataset to ensure a fair comparison.

Table 2. The obtained statistical results

Model	MAE (W/m²)	RMSE (W/m²)	nMAE (%)	nRMSE (%)	R² Score	R
CNN	302.87	378.15	18.55	23.17	0.841	0.917
LSTM	259.45	319.23	15.89	19.56	0.891	0.943
CNN-LSTM	228.56	289.24	13.99	17.74	0.916	0.957

As evidenced by the comparative results in Table 2, our experimental evaluation establishes a distinct performance hierarchy among the tested architectures, with the CNN-LSTM hybrid model significantly outperforming both standalone CNN and LSTM architectures across all evaluation metrics. The CNN model demonstrates a reasonable ability to identify short-term temporal patterns but is limited in capturing the sequential dependencies present in the solar radiation data. This limitation is evident in its relatively high RMSE and lower R² and correlation coefficient.
The LSTM model exhibits improved performance over the CNN by leveraging its strength in modeling temporal sequences. Its ability to capture long-range dependencies allows it to deliver more accurate predictions, as reflected by the reduction in MAE and RMSE. However, it still lacks the capability to efficiently extract localized features which can contribute to improved short-term estimations.
The CNN-LSTM model effectively combines the advantages of both architectures. It first uses CNN layers to extract robust localized features from input sequences, which are then processed by LSTM layers to model temporal dependencies over longer sequences. This hybrid structure allows the model to learn a richer representation of the underlying patterns in the solar radiation data.
Visual inspections in figure 9 of the predicted versus actual DNR and DSR values confirm the quantitative results. The CNN-LSTM predictions closely track the observed values, showing less fluctuation and lower residuals. In contrast, CNN predictions exhibit larger deviations during periods of high variability, while LSTM, although more consistent, sometimes underestimates peak values.

Journal of Information Systems Engineering and Management
2025, 10(4)
e-ISSN: 2468-4376
https://www.jisem-journal.com/

Research Article

Figure .9 simulate CNN-LSTM outputs for illustrative purposes.

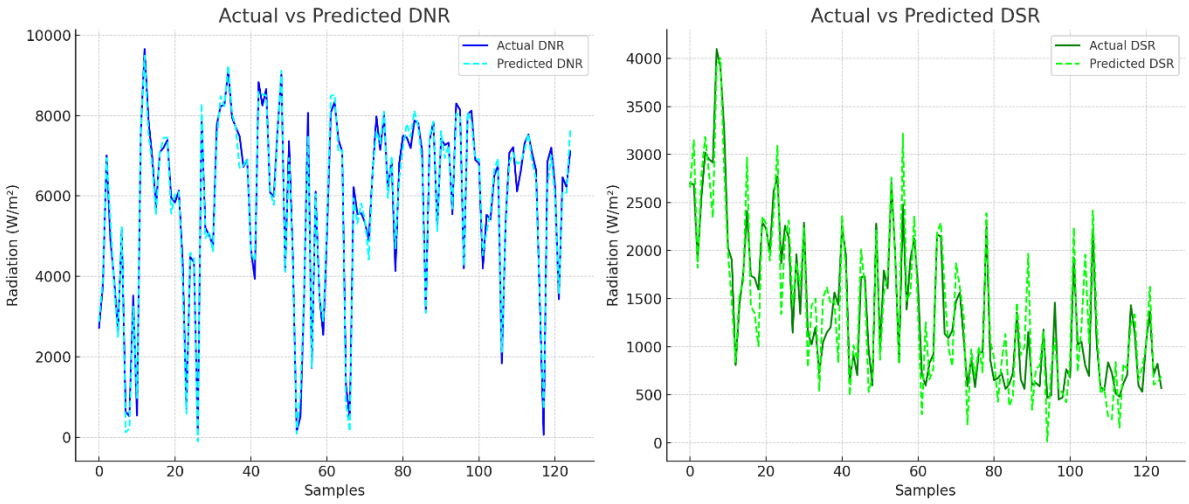

The superiority of the CNN-LSTM model is further emphasized by the normalized error metrics. With the lowest nMAE and nRMSE, it demonstrates not only high accuracy but also scalability and stability across different ranges of solar radiation intensity. The R^2 score of 0.916 and correlation coefficient of 0.957 indicate a strong linear relationship between predicted and actual values, which is crucial for real-time forecasting applications.

From a practical standpoint, these results suggest that the CNN-LSTM model can be confidently employed in solar energy forecasting systems where both short-term responsiveness and long-term accuracy are essential. The model's ability to generalize across diverse data patterns makes it suitable for deployment in different geographical locations and seasonal conditions. Future enhancements could involve the integration of additional meteorological inputs such as temperature, humidity, and cloud cover to further improve predictive performance.

CONCLUSION

This study demonstrates the effectiveness of CNN, LSTM, and their hybrid CNN-LSTM models in estimating DNR and DSR from GSR. Among them, the CNN-LSTM approach stands out due to its superior accuracy and capability in modeling both short-term and long-term temporal features. The approach successfully captures complex temporal and nonlinear relationships in the data, making it a valuable tool for solar energy forecasting and planning. Future work may include incorporating weather parameters and deploying the model for real-time prediction.

REFRENCES

[1] Mehallou, A., M'hamdi, B., Amari, A., Teguar, M., Rabehi, A., Guermoui, M., ... & Khafaga, D. S. (2025). Optimal multiobjective design of an autonomous hybrid renewable energy system in the Adrar Region, Algeria. Scientific Reports, 15(1), 4173.

[2] Boukredine, S., Mehallel, E., Boualleg, A., Baitiche, O., Rabehi, A., Guermoui, M., ... & Tibermacine, I. E. (2025). Enhanced Performance of Microstrip Antenna Arrays through Concave Modifications and Cut-Corner Techniques. ITEGAM-JETIA, 11(51), 65-71.

[3] Belaid, A., Guermoui, M., Riche, A., Arrif, T., Maamar, Rabehi, A., C. M., ... & Al Rahhal, M. M. (2024). High-Resolution Mapping of Concentrated Solar Power Site Suitability in Ghardaïa, Algeria: A GIS-Based Fuzzy Logic and Multi-Criteria Decision Analysis. IEEE Access.

[4] Younsi, A. M., Elbar, M., & Rabehi, A. (2024). Structural, Electronic, and Optical Properties of Perovskites CaATe3 (A= Zr Or Hf): A Theoretical Investigation. Semiconductors, 58(12), 984-992.

[5] Daha, R., Bouloudenine, M., Khiat, A., Gomez, C. V., La Pietra, M., Rabehi, A. E., ... & Bellucci, S. (2024). Enhancement of Cobalt Ferrite Properties through Rare Earth Ion Doping. Semiconductors, 58(12), 993-1005.

[6] Belaid, A., Guermoui, M., Khelifi, R., Arrif, T., Chekifi, T., Rabehi, A., ... & Alhussan, A. A. (2024). Assessing Suitable Areas for PV Power Installation in Remote Agricultural Regions. Energies, 17(22), 5792.

[7] Marzouglal, M., Souahlia, A., Bessissa, L., Mahi, D., Rabehi, A., Alharthi, Y. Z., ... & Ghoneim, S. S. (2024). Prediction of power conversion efficiency parameter of inverted organic solar cells using artificial intelligence techniques. Scientific Reports, 14(1), 25931.

[8] Ziane, A., Rabehi, A., Rouabhia, A., Amrani, M., Douara, A., Dabou, R., ... & Sahouane, N. (2024). Numerical Investigation of G–V Measurements of metal–A Nitride GaAs junction. Revista Mexicana de Física, 70(6 Nov-Dec), 061604-1.

[9] Mekaret, F., Rabehi, A., Zebentout, B., Tizi, S., Douara, A., Bellucci, S., ... & Alhussan, A. A. (2024). A comparative study of Schottky barrier heights and charge transport mechanisms in 3C, 4H, and 6H silicon carbide polytypes. AIP Advances, 14(11).

[10] Douara, A., Rabehi, A., Guermoui, M., Daha, R., & Tibermacine, I. E. (2024). Simulation-based optimization of barrier and spacer layers in InAlN/GaN HEMTs for improved 2DEG density. Micro and Nanostructures, 195, 207950.

[11] Rabehi, A., Douara, A., Mohamed, E., Zenzen, R., & Amrani, M. (2024). Impact of Grain Boundaries on The Electrical Characteristics and Breakdown Behavior of Polycrystalline Silicon Pin Diodes: A Simulation Study. ITEGAM-JETIA, 10(49), 59-64.

[12] Teta, A., Korich, B., Bakria, D., Hadroug, N., Rabehi, A., Alsharef, M., ... & Ghoneim, S. S. (2024). Fault detection and diagnosis of grid-connected photovoltaic systems using energy valley optimizer based lightweight CNN and wavelet transform. Scientific Reports, 14(1), 18907.

[13] Bouchakour, A., Zarour, L., Bessous, N., Bechouat, M., Borni, A., Rabehi, A., ... & Ghoneim, S. S. (2024). MPPT algorithm based on metaheuristic techniques (PSO & GA) dedicated to improve wind energy water pumping system performance. Scientific Reports, 14(1), 17891.

[14] Douara, A., Rabehi, A., Guermoui, M., Daha, R., & Tibermacine, I. E. (2024). Impact of AlN Buffer Layer Thickness on Electronic and Electrical Characteristics of In0. 17Al0. 83N/GaN High-Electron-Mobility Transistor. Physics of the Solid State, 66(6), 157-164.

[15] Ziane . A. Rabehi, A Numerical Investigation Of G–V Measurements Of metal – A Nitride GaAs junction, Revista Mexicana de Física, (accepted)

[16] Baitiche, O., Bendelela, F., Cheknane, A., Rabehi, A., & Comini, E. (2024). Numerical Modeling of Hybrid Solar/Thermal Conversion Efficiency Enhanced by Metamaterial Light Scattering for Ultrathin PbS QDs-STPV Cell. Crystals, 14(7), 668.

[17] Helal, H., Ahrouch, M., Rabehi, A., Zappa, D., & Comini, E. (2024). Nanostructured Materials for Enhanced Performance of Solid Oxide Fuel Cells: A Comprehensive Review. Crystals, 14(4), 306.

[18] Rabehi, A.; Helal, H.; Zappa, D.; Comini, E. Advancements and Prospects of Electronic Nose in Various Applications: A Comprehensive Review. Appl. Sci. 2024, 14, 4506. https://doi.org/10.3390/app14114506.

[19] Rabehi, A., Douara, A., Rabehi, A., Helal, H., Younsi, A. M., Amrani, M., ... & Benamara, Z. (2024). Accurate parameter estimation of Au/GaN/GaAs schottky diode model using grey wolf optimization. Revista Mexicana de Física, 70(2 Mar-Apr), 021004-1.

[20] El-Amarty, N., Marzouq, M., El Fadili, H., Bennani, SD., Ruano, A., Rabehi, A., A new evolutionary forest model via incremental tree selection for short-term global solar irradiance forecasting under six various climatic zones, Energy Conversion and Management, Volume 310,2024,118471, doi.org/10.1016/j.enconman.2024.118471.

[21] Ladjal, B., Tibermacine, I. E., Bechouat, M., Sedraoui, M., Napoli, C., Rabehi, A., & Lalmi, D. (2024). Hybrid models for direct normal irradiance forecasting: a case study of Ghardaia zone (Algeria). Natural Hazards, 1-23.

[22] Guermoui, M., Fezzani, A., Mohamed, Z., Rabehi, A., Ferkous, K., Bailek, N., ... & Ghoneim, S. S. (2024). An analysis of case studies for advancing photovoltaic power forecasting through multi-scale fusion techniques. Scientific Reports, 14(1), 6653.

[23] Teta, A., Medkour, M., Rabehi, A., Korich, B., & Bakria, D. (2024). Long-term solar radiation forecasting based on LSTM and attention mechanism: a case study in Algeria. Studies in Engineering and Exact Sciences, 5(1), 1117-1134.

[24] Behrang, M. A., Assareh, E., Ghanbarzadeh, A., & Noghrehabadi, A. R. (2010). The potential of different artificial neural network (ANN) techniques in daily global solar radiation modeling based on meteorological data. Solar Energy, 84(8), 1468-1480.

[25] Rahimikhoob, A. (2010). Estimating global solar radiation using artificial neural network and air temperature data in a semi-arid environment. Renewable energy, 35(9), 2131-2135.
[26] Yadav, A. K., & Chandel, S. S. (2014). Solar radiation prediction using Artificial Neural Network techniques: A review. Renewable and sustainable energy reviews, 33, 772-781.\
[27] Rehman, S., & Mohandes, M. (2008). Artificial neural network estimation of global solar radiation using air temperature and relative humidity. Energy policy, 36(2), 571-576.
[28] Lam, J. C., Wan, K. K., & Yang, L. (2008). Solar radiation modelling using ANNs for different climates in China. Energy conversion and management, 49(5), 1080-1090.
[29] Asl, S. F. Z., Karami, A., Ashari, G., Behrang, A., Assareh, A., & Hedayat, N. (2011). Daily global solar radiation modeling using multi-layer perceptron (MLP) neural networks. World Academy of Science, Engineering and Technology, 79, 740-742.
[30] Ramedani, Z., Omid, M., & Keyhani, A. (2013). Modeling solar energy potential in a Tehran province using artificial neural networks. International Journal of Green Energy, 10(4), 427-441.
[31] Mellit, A., & Pavan, A. M. (2010). A 24-h forecast of solar irradiance using artificial neural network: Application for performance prediction of a grid-connected PV plant at Trieste, Italy. Solar energy, 84(5), 807-821.
[32] Voyant, C., Muselli, M., Paoli, C., & Nivet, M. L. (2011). Optimization of an artificial neural network dedicated to the multivariate forecasting of daily global radiation. Energy, 36(1), 348-359.
[33] Koca, A., Oztop, H. F., Varol, Y., & Koca, G. O. (2011). Estimation of solar radiation using artificial neural networks with different input parameters for Mediterranean region of Anatolia in Turkey. Expert Systems with Applications, 38(7), 8756-8762.
[34] Khelifi, R., Guermoui, M., Rabehi, A., Taallah, A., Zoukel, A., Ghoneim, S. S., ... & Zaitsev, I. (2023). Short-Term PV Power Forecasting Using a Hybrid TVF-EMD-ELM Strategy. International Transactions on Electrical Energy Systems, 2023.
[35] Rabehi, A., Rabehi, A., & Guermoui, M. (2021). Evaluation of Different Models for Global Solar Radiation Components Assessment. Applied Solar Energy, 57(1), 81-92.
[36] Guermoui, M., Boland, J., & Rabehi, A. (2020). On the use of BRL model for daily and hourly solar radiation components assessment in a semiarid climate. The European Physical Journal Plus, 135(2), 1-16.
[37] Krizhevsky, A., Sutskever, I., & Hinton, G. E. (2017). ImageNet classification with deep convolutional neural networks. Communications of the ACM, 60(6), 84-90.
[38] Lu, W., Li, J., Wang, J., & Qin, L. (2021). A CNN-BiLSTM-AM method for stock price prediction. Neural Computing and Applications, 33(10), 4741-4753.
[39] Guermoui, M., Abdelaziz, R., Gairaa, K., Djemoui, L., & Benkaciali, S. (2022). New temperature-based predicting model for global solar radiation using support vector regression. International Journal of Ambient Energy, 43(1), 1397-1407.
[40] Helal, H., Benamara, Z., Kacha, A. H., Amrani, M., Rabehi, A., Akkal, B., ... & Robert-Goumet, C. (2019). Comparative study of ionic bombardment and heat treatment on the electrical behavior of Au/GaN/n-GaAs Schottky diodes. Superlattices and Microstructures, 135, 106276.
[41] Douara, A., Rabehi, A., Djellouli, B., Ziane, A., & Abid, H. (2021). 2-D optimisation current–voltage characteristics in AlGaN/GaN HEMTs with influence of passivation layer. International Journal of Ambient Energy, 42(12), 1363-1366.
[42] Lalmi, D., Benseddik, A., Bensaha, H., Bouzaher, M. T., Arrif, T., Guermoui, M., & Rabehi, A. (2021). Evaluation and estimation of the inside greenhouse temperature, numerical study with thermal and optical aspect. International Journal of Ambient Energy, 42(11), 1269-1280.
[43] A. Rabehi, M. Amrani, Z. Benamara, A. Ziane, B. Akkal, A. H. Kacha, C. Robert-Goumet,
[44] G. Monier, Gruzza. (2018). Simulation and experimental studies of illumination effects on the current transport of nitridated GaAs Schottky diode. Semiconductors,Vol. 52, No. 16, pp. 1996–2004.
[45] Rabehi, A., Guermoui, M., khelifi, R., & Mekhalfi, M. L. (2018). Decomposing Global Solar Radiation into its Diffuse and Direct Normal Radiation. International Journal of Ambient Energy, DOI: 10.1080/01430750.2018.1492445.
[46] Rabehi, A., Guermoui, M., & Lalmi, D. (2018). Hybrid models for global solar radiation prediction: a case study. International Journal of Ambient Energy, 1-10.

[47] Douara, A., Djellouli, B., Abid, H., Rabehi, A., Ziane, A., Mostefaoui, M., ... & Dif, N. (2018). Optimization of two-dimensional electron gas characteristics of AlGaN/GaN high electron mobility transistors. Int J Numer Model. 2018; e 2518. Doi: 10.1002/jnm.2518.

[48] Ziane, A., Amrani, M., Rabehi, A., & Benamara, Z. (2018). Low-and High-Frequency CV Characteristics of Au/N-GaN/N-GaAs. International Journal of Nanoscience. doi:10.1142/S0219581X18500394.

[49] Guermoui, M., & Rabehi, A. (2018). Soft Computing for Solar Radiation Potential Assessment in Algeria. International Journal of Ambient Energy, DOI: 10.1080/01430750.2018.1517686.

[50] khelifi, R., Guermoui, M., Rabehi, A., & Lalmi, D. (2018). Multi-Step Ahead Forecasting of Daily Solar Radiation Components in Saharan Climate. International Journal of Ambient Energy, DOI: 10.1080/01430750.2018.1490349.

[51] Guermoui, M., Gairaa, K., Rabehi, A., Djafer, D., & Benkaciali, S. (2018). Estimation of the daily global solar radiation based on the Gaussian process regression methodology in the Saharan climate. The European Physical Journal Plus, 133(6), 211.

[52] Harzallah, S., Rebhi, R., Chabaat, M., Rabehi, A., Eddy current modelling using multilayer perceptron neural networks for detecting surface cracks, Frattura ed Integrità Strutturale, 45 (2018) 147-155.

[53] Lalmi, D., Bezari, S., Bensaha, H., Guermouai, M., Rabehi, A., Abdelouahab, B., & Hadef, R. Analysis of thermal performance of an agricultural greenhouse heated by a storage system (2018). Modelling, Measurement and Control B. Journal homepage: http://iieta. org/Journals/MMC/MMC_B, 87(1), 15-20.

[54] Ziane, A., Amrani, M., Benamara, Z., & Rabehi, A. (2018). Modeling and Simulation of Capacitance–Voltage Characteristics of a Nitride GaAs Schottky Diode. Journal of Electronic Materials, DOI 10.1007/s11664-018-6408-1.

[55] Guermoui, M., Rabehi, A., Gairaa, K., & Benkaciali, S. (2018). Support vector regression methodology for estimating global solar radiation in Algeria. The European Physical Journal Plus,133(1), 22.

[56] Helal, H., Benamara, Z., Kacha, A. H., Rabehi, A., Akkal, B., & Amrani, M. (2017, October). Electron cyclotron resonance ion source nitridation of Au/n-GaAs schottky diode and current- voltage characterization. In Electrical Engineering-Boumerdes (ICEE-B), 2017 5th International Conference on (pp. 1-6). IEEE.

[57] RABEHI, A., GUERMOUI, M., & MIHOUB, R. (2017). Direct and diffuse solar radiation components estimation based on RBF model: Case study. Leonardo Electronic Journal of Practices and Technologies, (31), 93-110.

[58] Rabehi, A., Amrani, M., Benamara, Z., Akkal, B., & Kacha, A. H. (2016). Electrical and photoelectrical characteristics of Au/GaN/GaAs Schottky diode. Optik-International

[59] Journal for Light and Electron Optics, 127(16), 6412-6418.

[60] A. Rabehi, M Guermoui, D Djafer, et al. Radial basis function neural networks model to estimate global solar radiation in semi-arid area. Leonardo Electronic Journal of Practices and Technologies, 2015, no 27, p. 177-184.

[61] Rabehi, A., Amrani, M., Benamara, Z., Akkal, B., Hatem-Kacha, A., Robert-Goumet, C., ... & Gruzza, B. (2015). Study of the characteristics current-voltage and capacitance-voltage in nitride GaAs Schottky diode. The European Physical Journal Applied Physics, 72(1), 10102.

[62] Guermoui, M., Rabehi, A., Benkaciali, S., & Djafer, D. (2016). Daily global solar radiation modelling using multi-layer perceptron neural networks in semi-arid region. Leonardo Electronic Journal of Practices and Technologies, 28, 35-46.

[63] Kacha, A. H., Akkal, B., Benamara, Z., Amrani, M., Rabehi, A., Monier, G., ... & Gruzza,

[64] B. (2015). Effects of the GaN layers and the annealing on the electrical properties in the Schottky diodes based on nitrated GaAs. Superlattices and Microstructures, 83, 827-833.

[65] Younsi, A,M,. Rabehi, A. (2023). Ab-initio study on structural, magnetic, electronic and optical properties of SrCo1−xAxO3 (A = Fe or Cr, x = 0.125 and 0.25). Modern Physics Letters B. doi: 10.1142/S0217984924500556.

[66] Douara, A., Rabehi, A., Baitiche, O., & Handami, M. (2023). Improved electrical characteristics of AlxGa1−xN/GaN High Electron Mobility Transistor by effect of physical and geometrical parameters. Revista Mexicana de Física, 69(4 Jul-Aug), 041001-1.

[67] Douara, A., Rabehi, A., & Baitiche, O. (2023). Impact of AlN interlayer on the electronic and IV characteristics of In0. 17Al0. 83N/GaN HEMTs devices. Revista mexicana de física, 69(3), 0-0.

[68] Rabehi, A., Rabehi, A., Douara, A., Helal, H., Baitiche, O., Akkal, B., ... & Benamara, Z. (2022). Modeling the Abnormal Behavior of the 6H-SiC Schottky Diode Using Lambert W Function. Journal of Nano-and Electronic Physics, 14(6).

[69] Bekaddour, A., Rabehi, A., Tizi, S., Zebentout, B., Akkal, B., & Benamara, Z. (2022). Effect of the contact area on the electrical characteristics of the Ti/6H−SiC (n) Schottky diode. Micro and Nanostructures, 207464.

[70] Helal, H., Benamara, Z., Comini, E., Kacha, A. H., Rabehi, A., Khirouni, K., ... & Dominguez, M. (2022). A new approach to studying the electrical behavior and the inhomogeneities of the Schottky barrier height. The European Physical Journal Plus, 137(4), 450.

[71] Rabehi, A., Rabehi, A., & Guermoui, M. (2021). Evaluation of Different Models for Global Solar Radiation Components Assessment. Applied Solar Energy, 57(1), 81-92.

[72] Helal, H., Benamara, Z., Wederni, M. A., Mourad, S., Khirouni, K., Monier, G., Rabehi A, ... & Dominguez, M. (2021). Conduction Mechanisms in Au/0.8 nm−GaN/n−GaAs Schottky Contacts in a Wide Temperature Range. Materials, 14(20), 5909.

[73] Rabehi A, Akkal B, Amrani M, Tizi S, Benamara Z, Helal H, Douara A, Nail B, Ziane A. Current--Voltage, Capacitance--Voltage--Temperature, and DLTS Studies of Ni|6H-SiC Schottky Diode. Semiconductors, DOI: 10.21883/FTP.2021.04.50744.9541A

[74] Ziane, A., Amrani, M., Rabehi, A., Douara, A., Mostefaoui, M., Necaibia, A., Sahouane, N., Dabou, R. and Bouraiou, A., 2021. Frequency Dependent Capacitance and Conductance–Voltage Characteristics of Nitride GaAs Schottky Diode. Semiconductors, 55(1), pp.51-55.

[75] Helal, H., Benamara, Z., Arbia, M.B., Rabehi, A., Chaouche, A.C. and Maaref, H., 2021. Electrical behavior of n-GaAs based Schottky diode for different contacts: Temperature dependence of c urrent-voltage. International Journal of Numerical Modelling: Electronic Networks, Devices and Fields, p.e2916.

[76] Rabehi, A., Nail, B., Helal, H., Douara, A., Ziane, A., Amrani, M., ... & Benamara, Z. (2020). Optimal Estimation of Schottky Diode Parameters Using Advanced Swarm Intelligence Algorithms. Semiconductors, 54(11), 1398-1405.

[77] Helal, H., Benamara, Z., Pérez, B. G., Kacha, A. H., Rabehi, A., Wederni, M. A., ... & Robert- Goumet, C. (2020). A new model of thermionic emission mechanism for non-ideal Schottky contacts and a method of extracting electrical parameters. The European Physical Journal Plus, 135(11), 1-14